PHYSICAL REVIEW D

PARTICLES AND FIELDS

THIRD SERIES, VOLUME 33, NUMBER 2 15 JANUARY 1986

Superconducting inductance-bridge transducer for resonant-mass gravitational-radiation detector

Ho Jung Paik*

Department of Physics, Stanford University, Stanford, California 94305

(Received 18 July 1985)

The sensitivity of cryogenic gravitational-radiation detectors is presently limited by the performance of the transducers. A superconducting ac-pumped inductance bridge is proposed as a new transducer for resonant-mass gravitational-radiation detectors. The impedance matrix of the transducer is computed to determine the input, output, and transfer characteristics of the electromechanical system. It is shown that the dissipative forces exerted on the proof mass by the bridge circuit through the two sidebands cancel each other almost exactly so that the Brownian-motion level is nearly unaffected by the electric sensing circuit. This implies that an effective energy coupling coefficient near unity could be used without being limited by the electrical Nyquist noise. With the parametric up conversion of the signal, the inductance bridge can be coupled to a nearly quantum-limited dc superconducting quantum interference device (SQUID). The sensitivity of the gravitational-radiation detector employing the new superconducting transducer is computed as a function of transducer parameters. It is shown that the proposed transducer, with modest values for its parameters, is capable of matching a high-Q gravitational-radiation antenna, cooled to 50 mK, to a nearly quantum-limited dc SQUID.

I. INTRODUCTION

An extremely low-noise transducer with high electromechanical energy coupling is required for a sensitive resonant-mass gravitational-radiation detector. In order to improve beyond the performance of piezoelectric transducers originally employed for Weber's room-temperature antennas,[1] various passive and active transducers have been developed for cryogenic gravitational-radiation detectors.[2]

In a *passive* transducer, the mechanical motion of the proof mass modulates dc energy in the electrical circuit so that the output signal remains at the input-signal frequency ω_m. In an *active* transducer, however, the electrical circuit is driven at a pump frequency $\omega_p \gg \omega_m$ and the output signal appears at the two sidebands $\omega_\pm$, where

$$\omega_\pm \equiv \omega_p \pm \omega_m \ . \tag{1}$$

The dc-voltaged-biased capacitor transducer[3,4] and the superconducting inductive transducer,[5] in which a persistent current is used for the dc current bias, fall in the first category. A *resonant* LC circuit or a *resonant* cavity is usually employed for the second class of transducers in order to take advantage of the signal gain by the electrical Q at the pump frequency. Either the capacitive[6] or the inductive[7] component is modulated by the mechanical motion in the LC circuit transducer, and the capacitance is modulated in the reentrant cavity transducer.[8-11]

Since modulation of the resonance frequency is the signal coupling mechanism in a *resonant* active transducer, the frequency noise of the external oscillator is an important source of noise.[6,12] In order to reduce the effect of this oscillator noise, one employs a superconducting cavity stabilized oscillator (SCSO) (Refs. 9 and 10) or balances out the pump noise by matching two resonant cavities[8,11] or LC circuits.[13]

In this paper we propose a simpler form of active transducer: a *superconducting inductance bridge.* The four bridge inductances are modulated mechanically at ω_m and the bridge is driven electrically at $\omega_p \gg \omega_m$. No electrical resonances are introduced so that the pump signal is *amplitude modulated* by the mechanical motion. The large carrier signal at ω_p is precisely balanced at the bridge by applying a feedback force to the proof mass. This "force rebalance" operation not only improves the dynamic range of the system, but virtually eliminates the oscillator noise at the bridge output. The absence of capacitance and the low loss in the superconducting bridge should make the bridge balance relatively straightforward. Further, the all-inductance bridge is an ideal input circuit for the most sensitive amplifier known today, the dc SQUID (superconducting quantum interference device). Nearly quantum-limited dc SQUID's exhibit $1/f$ noise below 100 kHz (Ref. 14), which presents a problem for the passive

superconducting transducer.[5] In the active bridge transducer, this problem is bypassed by choosing ω_p above the $1/f$ noise corner frequency.

The input, output, and transfer characteristics of a transducer can be completely determined by means of an *impedance matrix*. We would like to obtain the impedance matrix Z_{ij} of the form given by

$$\begin{bmatrix} V_-^* \\ F_1 \\ V_+ \end{bmatrix} = \begin{bmatrix} Z_{--}^* & Z_{-1}^* & 0 \\ Z_{1-} & Z_{11} & Z_{1+} \\ 0 & Z_{+1} & Z_{++} \end{bmatrix} \begin{bmatrix} I_-^* \\ U_1 \\ I_+ \end{bmatrix} , \tag{2}$$

where the input variables F_1 and U_1 are the force and velocity and the output variables $V_\pm$ and $I_\pm$ represent the voltages and currents at the two sidebands $\omega_\pm$. We follow the approach outlined by Giffard and Paik[15] to compute all the matrix elements. The pulse detection noise temperature[16] of the entire gravitational-radiation detector is then computed in terms of these transducer parameters. It is found that the electrical damping terms at the two sidebands $\omega_\pm$ nearly cancel each other. This suggests a possibility of increasing the energy coupling coefficient without incurring excessive electrical losses at the mechanical frequency ω_m. The relatively low electrical Q of the passive transducers, including the superconducting inductive transducer ($Q_e \lesssim 10^5$, typically), tends to increase the thermal noise of the antenna in the high coupling limit. Thus the useful value of the energy coupling coefficient is presently limited to approximately 10^{-2} in the passive transducers.[16] This situation could be improved by means of the proposed active transducer.

II. DYNAMICS OF THE TRANSDUCER

The superconducting inductance-bridge transducer is schematically shown in Fig. 1. Also shown in the figure is an equivalent circuit of the SQUID with two conjugate noise sources: S_e and S_i. The bridge formed by four inductors, L_1, L_2, L_3, and L_4, is driven by an external oscillator with an ac current across AB:

$$i_0(t)=\mathrm{Re}(I_0 e^{j\omega_p t})=I_0\cos\omega_p t \ . \tag{3}$$

Let the bridge inductances be modulated by a displacement of the proof mass, $x(t)$, according to

$$L_1(t)=L_1^0[1+x(t)/d_1^0]=L_1^0+\Lambda x(t) \ , \tag{4a}$$

$$L_2(t)=L_2^0[1-x(t)/d_2^0]=L_2^0-\Lambda x(t) \ , \tag{4b}$$

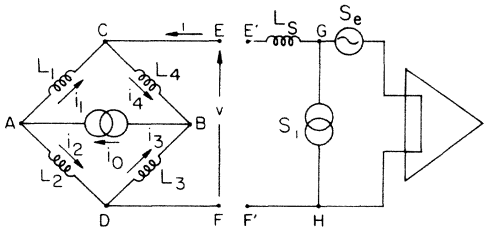

FIG. 1. A schematic circuit diagram of the superconducting inductance-bridge transducer and an equivalent circuit of a dc SQUID.

$$L_3(t)=L_3^0[1+x(t)/d_3^0]=L_3^0+\Lambda x(t) \ , \tag{4c}$$

$$L_4(t)=L_4^0[1-x(t)/d_4^0]=L_4^0-\Lambda x(t) \ , \tag{4d}$$

where $d_k^0 (k=1,\ldots,4)$ is the equilibrium value of the spacing d_k for the coil L_k and where the geometry of the sensing coils has been assumed to be identical:

$$L_1^0/d_1^0=L_2^0/d_2^0=L_3^0/d_3^0=L_4^0/d_4^0\equiv\Lambda \ . \tag{5}$$

This assumption simplifies analysis and is satisfied reasonably well in practical pancake-shaped sensing coils. It will be seen, however, that the conclusions of this paper do not depend on this condition.

The input variables chosen in Eq. (2) are the velocity of the proof mass, $u(t)$, and the force acting on it, $f(t)$:

$$u(t)=\mathrm{Re}(U_1 e^{j\omega_m t})=U_1\cos\omega_m t \ , \tag{6}$$

$$f(t)=\mathrm{Re}(F_0+F_1 e^{j\omega_m t}) \ . \tag{7}$$

From Eq. (6), one finds

$$x(t)=(U_1/\omega_m)\sin\omega_m t \ , \tag{8}$$

which can be substituted into Eqs. (4) to express $L_x(t), k=1,\ldots,4$, in terms of U_1.

In this section, we will ignore the effect of electrical damping on the bridge operation. Four independent circuit equations can then be written as

$$L_1(t)i_1(t)-L_2(t)i_2(t)-L_3(t)i_3(t)+L_4(t)i_4(t)=0 \ , \tag{9a}$$

$$i_1(t)+i_2(t)=i_0(t) \ , \tag{9b}$$

$$-i_1(t)+i_4(t)=i(t) \ , \tag{9c}$$

$$i_2(t)-i_3(t)=i(t) \ . \tag{9d}$$

Simultaneous solution of these equations gives

$$i_1(t)=D^{-1}[(L_2+L_3)i_0-(L_3+L_4)i] \ , \tag{10a}$$

$$i_2(t)=D^{-1}[(L_1+L_4)i_0+(L_3+L_4)i] \ , \tag{10b}$$

$$i_3(t)=D^{-1}[(L_1+L_4)i_0-(L_1+L_2)i] \ , \tag{10c}$$

$$i_4(t)=D^{-1}[(L_2+L_3)i_0+(L_1+L_2)i] \ , \tag{10d}$$

where the time dependence of the current variables and inductances have been omitted on the right-hand sides of Eqs. (10) and

$$\begin{aligned} D&\equiv L_1(t)+L_2(t)+L_3(t)+L_4(t) \\ &=L_1^0+L_2^0+L_3^0+L_4^0 \ . \end{aligned} \tag{11}$$

The output voltage is then obtained from

$$v(t)=(d/dt)[L_2(t)i_2(t)-L_1(t)i_1(t)] \ . \tag{12}$$

The output variables are expected to have the form

$$i(t)=\mathrm{Re}(I_p e^{j\omega_p t}+I_+ e^{j\omega_+ t}+I_- e^{j\omega_- t}) \ , \tag{13}$$

$$v(t)=\mathrm{Re}(V_p e^{j\omega_p t}+V_+ e^{j\omega_+ t}+V_- e^{j\omega_- t}) \ . \tag{14}$$

Substituting Eqs. (3), (10), (13), and (14) into Eq. (12) and identifying terms that involve the same time dependences on the two sides of Eq. (12), one finds

$$V_p = D^{-1}(L_2^0 L_4^0 - L_1^0 L_3^0) j\omega_p I_0 + D^{-1}(L_1^0 + L_2^0)(L_3^0 + L_4^0) j\omega_p I_p \ , \quad (15a)$$

$$V_\pm = \mp(\Lambda I_0 U_1/2)(\omega_\pm/\omega_m) + D^{-1}(L_1^0 + L_2^0)(L_3^0 + L_4^0) j\omega_\pm I_\pm \ , \quad (15b)$$

to the leading order in the modulation depth $U_1/(\omega_m d_i^0)$. Here the condition (5) has been used to simplify the first term of Eq. (15b).

Equations (15) determine the forward transfer and output characteristics of the transducer. In order to complete the analysis, we compute the effect of the electric circuit on the mechanical motion of the transducer, i.e., the reverse transfer and input characteristics of the instrument. The electromagnetic force acting on the proof mass is given by

$$f(t) = L_1 i_1^2/2d_1 - L_2 i_2^2/2d_2 + L_3 i_3^2/2d_3 - L_4 i_4^2/2d_4 = (\Lambda/2)[(i_1+i_2)(i_1-i_2)+(i_3+i_4)(i_3-i_4)] \ , \quad (16)$$

where use was made of Eq. (5) and the time dependence of the current variables are implied. Substitution of Eqs. (10) and Eq. (16) leads to

$$f(t) = -\Lambda i_0(t) i(t) = -(\Lambda I_0/2)\mathrm{Re}[I_p + (I_+ + I_-^*)e^{j\omega_m t}] \ , \quad (17)$$

where terms with frequencies of the order of $2\omega_p$ have been ignored. Comparing this with Eq. (7), one finds

$$F_0 = -(\Lambda I_0/2) I_p \ , \quad (18a)$$

$$F_1 = -(\Lambda I_0/2)(I_+ + I_-^*) \ . \quad (18b)$$

The elements of the impedance matrix are read off Eqs. (15) and (18) in the following section.

Notice that the condition (5) led to the simple coupling coefficient $\Lambda I_0/2$ in Eqs. (15) and (18). When this condition is not satisfied, the coupling coefficient has a general form involving L_k/d_k for $k = 1, \ldots, 4$. Essential features of the transducer clearly remain the same. Notice also that the bridge balance condition,

$$\epsilon_b \equiv \frac{L_4^0}{L_3^0} - \frac{L_1^0}{L_2^0} = 0 \ , \quad (19)$$

has not been assumed in the derivation of the equations in this section. This additional condition eliminates the first term in Eq. (15a), the pump signal leaking through to the transducer output. It is desirable to maintain the balance at all times by operating the instrument in a negative feedback mode so that the bridge becomes a *null* detector for a proof mass displacement away from its balance point. Then the oscillator noise is balanced out along with the carrier signal and the dynamic range of the instrument is improved.

Figure 2 is a schematic circuit diagram of the "force rebalanced" bridge transducer. The driving current from an external oscillator is amplified through a resonant tank circuit which is coupled to the bridge through a superconducting transformer with a step-down turns ratio. After detecting the sidebands with a dc SQUID and demodulating them, the input frequency signal is fed back through a voltage-to-current converter to a forcing coil loop carrying a bias dc current I_b. The relative positions of the sensing and feedback coils, L_1 through L_6, are shown in Fig. 3. In the force rebalance mode, the demodulated output signal is a direct measure of the specific force or acceleration applied to the transducer.

III. IMPEDANCE MATRIX AND ENERGY COUPLING COEFFICIENTS

Equations (15) show that the input velocity U_1 generates signal voltages only at the two sidebands, $V_\pm$, which in turn induce sideband currents $I_\pm$ to flow through the amplifier input. The first term of Eq. (15b) yields the *forward transductances* $Z_{\pm 1}$:

$$Z_{\pm 1} = \mp(\Lambda I_0/2)(\omega_\pm/\omega_m) \ . \quad (20)$$

The second terms in Eqs. (15) represent the voltages across the transducer output due to currents I_p and $I_\pm$ impressed at the output terminals. The output impedances $Z_{\pm\pm}$ are given by the ratio of these voltages to $I_\pm$:

$$Z_{\pm\pm} = j\omega_\pm L_0 \ , \quad (21)$$

where L_0 is the total bridge inductance seen across the output terminals:

$$L_0^{-1} = (L_1^0 + L_2^0)^{-1} + (L_3^0 + L_4^0)^{-1} \ . \quad (22)$$

The residual component of V_p, after balance, produces a dc bias upon demodulation and is filtered out in the signal processing. Therefore, we can ignore V_p as long as it does not overload the amplifier.

The *reverse transductances* $Z_{1\pm}$ are read off Eq. (18b):

$$Z_{1\pm} = -\Lambda I_0/2 \ . \quad (23)$$

Notice that the output current at the pump frequency, I_p, produces a dc force, which is not relevant for our discussion. When the symmetric coil condition, Eq. (5), is not satisfied, there is in general an additional term in F_0, which is proportional to I_0^2. The amplitude fluctuations in I_0 at the frequencies $\omega_\pm$ can then contribute to the back action noise of the circuit.

In order to compute the *input impedance* Z_{11}, one needs to find the force F_1 generated by the circuit in response to the input velocity U_1. Equation (18b) gives the relationship between F_1 and the output currents $I_\pm$. Hence, one

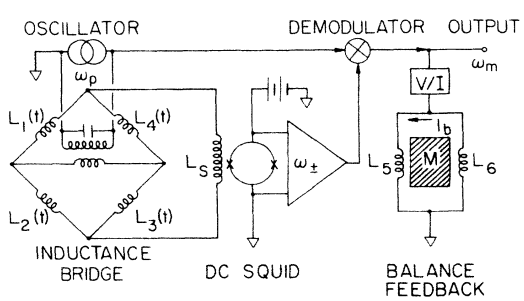

FIG. 2. A schematic diagram of the inductance-bridge transducer with force rebalance feedback.

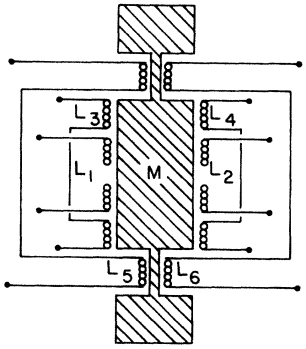

FIG. 3. Relative positions of the sensing and feedback coils.

can find Z_{11} from Eq. (18b) by substituting $I_{\pm}$, which are generated by U_1. Since $I_{\pm}=0$ with the transducer output open circuited, it is clear that the functional dependence of $I_{\pm}$ on U_1 depends on the load impedance connected to the transducer output. We therefore consider the case in which a SQUID with an input coil inductance L_S is connected at the output of the bridge. A SQUID can be represented[17–19] by an ideal current amplifier with zero input impedance in series with a stray inductance L_S, as is seen in Fig. 1. The output voltages $V_{\pm}$ are then given by the back emf:

$$V_{\pm}=-j\omega_{\pm}L_S I_{\pm} . \tag{24}$$

Substituting this into Eqs. (15), one obtains

$$I_{\pm}=\pm[j\omega_m L_0(1+\gamma)]^{-1}(\Lambda I_0/2)U_1 , \tag{25}$$

where

$$\gamma\equiv L_S/L_0 . \tag{26}$$

Combining Eq. (25) with Eq. (18b), one finds

$$Z_{11}=-\frac{2}{1+\gamma}\left[\frac{\Lambda I_0}{2}\right]^2\frac{1}{j\omega_m L_0} . \tag{27}$$

This completes derivation of the matrix elements Z_{ij}. It is clear that the particular choice of variables in Eq. (2) with complex conjugates in the first row has been necessitated by Eq. (18b) which relates F_1 to I_+ and I_-^*. Equation (27) implies that the transducer proof mass experiences an additional positive spring constant

$$k_E=\frac{2}{1+\gamma}\left[\frac{\Lambda I_0}{2}\right]^2\frac{1}{L_0} , \tag{28}$$

due to the presence of the magnetic field.

It is instructive to compare the matrix elements, Eqs. (20), (21), (23), and (27), with the corresponding quantities for other passive and active transducers. In Table I we show the impedance matrix elements Z_{ij} and the "energy coupling coefficients" β for the present transducer and for four other types of transducers, computed earlier.[2] In the passive capacitor transducer, C and E_0 are the sensing capacitance and the applied dc electric field, whereas, in the passive inductance transducer, L_0 and I_0 represent the output inductance and the stored dc current of the sensing circuit. The inductance modulation coefficient Λ, defined by Eq. (5) for each sensing coil, appears in all three inductance-modulated transducers. In the capacitance-modulated resonator, C and E_p are the sensing capacitance and the amplitude of the electric field at the pump frequency. Likewise, in the inductance-modulated resonator, L and I_p are the sensing inductance and the amplitude of the pump current flowing through L, respectively. In both circuits, Q and $\Delta_{\pm}$ represent the quality factor of the resonator and the frequency tuning parameter defined by

$$\Delta_{\pm}\equiv 2^{-1}(\omega_{\pm}/\omega_0-\omega_0/\omega_{\pm}) , \tag{29}$$

where $\omega_{\pm}$ are given by Eq. (1) and ω_0 is the resonance frequency of the circuit, which does not necessarily coincide with ω_p. When both sidebands are detected, the total input impedance Z_{11} and the total energy coupling coefficient β can be obtained by summing their respective sideband components.

The transducer energy coupling coefficients $\beta_{\pm}$ are defined as the geometric means of the "forward and reverse energy coupling coefficients," $\beta_{\pm 1}$ and $\beta_{1\pm}$:

$$\beta_{\pm}\equiv(\beta_{\pm 1}\beta_{1\pm})^{1/2} , \tag{30a}$$

where

$$\beta_{\pm 1}\equiv\frac{|Z_{\pm 1}|^2}{M\omega_m|Z^L_{\pm\pm}|} , \tag{30b}$$

$$\beta_{1\pm}\equiv\frac{|Z_{1\pm}|^2}{M\omega_m|Z^L_{\pm\pm}|} . \tag{30c}$$

Here M is the dynamic mass of the transducer, and $Z^L_{\pm\pm}$ are the "loaded output impedances" which include the effect of the input impedance of the amplifier. For the transducer with an output inductance L_0, which is followed by a SQUID with an input inductance L_S, $Z^L_{\pm\pm}$ become

$$Z^L_{\pm\pm}=j\omega_{\pm}L_0(1+\gamma) , \tag{31}$$

where γ is the parameter defined by Eq. (26). For the inductance-bridge transducer, the energy-coupling coefficients are therefore given by

$$\beta_{\pm 1}=\frac{\omega_{\pm}}{\omega_m}\frac{1}{1+\gamma}\frac{(\Lambda I_0/2)^2}{M\omega_m{}^2L_0} , \tag{32a}$$

$$\beta_{1\pm}=\frac{\omega_m}{\omega_{\pm}}\frac{1}{1+\gamma}\frac{(\Lambda I_0/2)^2}{M\omega_m{}^2L_0} , \tag{32b}$$

$$\beta_{\pm}=\frac{1}{1+\gamma}\frac{(\Lambda I_0/2)^2}{M\omega_m{}^2L_0} . \tag{32c}$$

The relevance of these coefficients will be made clear in Sec. V, where we discuss the overall sensitivity of the gravitational-radiation detector.

Table I reveals that the inductance bridge resembles the modulated resonator transducers in that it has parametric gains:

$$G_p^{\pm}=|Z_{\pm 1}/Z_{1\pm}|=\omega_{\pm}/\omega_m\cong\omega_p/\omega_m , \tag{33}$$

although there is no signal gain by the Q of the resonance

TABLE I. Impedance matrix elements and energy-coupling coefficients for various transducers. Effects of electrical damping have been ignored in the passive transducers and the inductance-bridge transducer.

Type of transducer	Impedance matrix elements Z_{11}	Z_{12}	Z_{21}	Z_{22}	Energy coupling coefficient β
Capacitor (passive)	$\frac{(CE_0)^2}{j\omega_m}$	$\frac{E_0}{j\omega_m}$	$\frac{E_0}{j\omega_m}$	$\frac{1}{j\omega_m C}$	$\frac{CE_0{}^2}{M\omega_m{}^2}$
Inductor (passive)	$-\frac{1}{1+\gamma}\frac{(\Lambda I_0)^2}{j\omega_m L_0}$	ΛI_0	$-\Lambda I_0$	$j\omega_m L_0$	$\frac{1}{1+\gamma}\frac{(\Lambda I_0)^2}{M\omega_m{}^2 L_0}$
Capacitance-modulated resonator (active)	$\pm\frac{\omega_\pm}{\omega_m}\frac{(CE_p)^2 Q}{4\omega_0 C}$	$-\frac{E_p Q}{2\omega_0}$	$\mp\frac{\omega_\pm}{\omega_m}\frac{E_p Q}{2\omega_0}$	$\frac{Q}{\omega_0 C}$	$\frac{CE_p{}^2 Q}{4M\omega_m{}^2}$
	$\times\left[\frac{1\pm 2jQ\Delta_\pm}{1+4Q^2\Delta_\pm{}^2}\right]$	$\times\left[\frac{1\pm 2jQ\Delta_\pm}{1+4Q^2\Delta_\pm{}^2}\right]$	$\times\left[\frac{1-2jQ\Delta_\pm}{1+4Q^2\Delta_\pm{}^2}\right]$	$\times\left[\frac{1-2jQ\Delta_\pm}{1+4Q^2\Delta_\pm{}^2}\right]$	$\times\frac{\omega_\pm/\omega_0}{(1+4Q^2\Delta_\pm{}^2)^{1/2}}$
Inductance-modulated resonator (active)	$\mp\frac{\omega_\pm}{\omega_m}\frac{(\Lambda I_p/2)^2 Q}{\omega_0 L}$	$\mp\frac{\omega_\pm}{\omega_0}\frac{\Lambda I_p Q}{2}$	$\frac{\omega_0}{\omega_m}\frac{\Lambda I_p Q}{2}$	$\omega_0 LQ$	$\frac{(\Lambda I_p/2)^2 Q}{M\omega_m{}^2 L}$
	$\times\left[\frac{1\pm 2jQ\Delta_\pm}{1+4Q^2\Delta_\pm{}^2}\right]$	$\times\left[\frac{1\pm 2jQ\Delta_\pm}{1+4Q^2\Delta_\pm{}^2}\right]$	$\times\left[\frac{1-2jQ\Delta_\pm}{1+4Q^2\Delta_\pm{}^2}\right]$	$\times\left[\frac{1-2jQ\Delta_\pm}{1+4Q^2\Delta_\pm{}^2}\right]$	$\times\frac{\omega_\pm/\omega_0}{(1+4Q^2\Delta_\pm{}^2)^{1/2}}$
Inductance-bridge (active)	$-\frac{1}{1+\gamma}\frac{(\Lambda I_0/2)^2}{j\omega_m L_0}$	$-\frac{\Lambda I_0}{2}$	$\mp\frac{\omega_\pm}{\omega_m}\frac{\Lambda I_0}{2}$	$j\omega_\pm L_0$	$\frac{1}{1+\gamma}\frac{(\Lambda I_0/2)^2}{M\omega_m{}^2 L_0}$

and the device is similar to the passive inductor transducer in many other respects. As we will see in Sec. V, the parametric up conversion permits operation of a nearly quantum-limited dc SQUID in its white-noise region.

IV. EFFECTS OF ELECTRICAL DISSIPATION

In this section we consider effects of electrical damping on the previous analysis. In a superconducting circuit, ac losses can occur from a number of sources: irreversible flux flow,[20] dielectric loss in the insulating material,[21] eddy current damping in a normal metal, induced motion of the coil, etc. Since the electric loss occurs at either the fundamental or second harmonic of the driving frequency in all these mechanisms, the dissipation can be modeled as a resistor in series with the inductor which gives the observed Q of the inductor at ω_p. Then, the sensing inductors L_k in Fig. 1 are replaced by L_k', where

$$L_k' \equiv L_k + r_k/j\omega = L_k[1-(j/Q_0)(\omega_p/\omega)] . \tag{34}$$

Here we assumed the same Q for the four inductors:

$$Q_0 = \omega_p L_k / r_k . \tag{35}$$

If the dissipation mechanism is a *thermodynamic process*, the equivalent resistor will be accompanied by a Nyquist noise generator according to the fluctuation-dissipation theorem.

We use a perturbation method to compute correction terms in Z_{ij}. The solution to the unperturbed equations has been obtained in Secs. II and III. It follows from Eqs. (9) that the first-order corrections to the currents $i_k(t)$ vanish as long as r_k and L_k satisfy the relationship (34). The first-order correction to the output voltage is then simply

$$\delta v(t) = r_2 i_2(t) - r_1 i_1(t) . \tag{36}$$

Substituting Eqs. (3), (10), (13), and (34) into this equation, one finds

$$\delta V_p = (\omega_p/Q_0) D^{-1}(L_2^0 L_4^0 - L_1^0 L_3^0) I_0 + (\omega_p/Q_0) D^{-1}(L_1^0 + L_2^0)(L_3^0 + L_4^0) I_p , \tag{37a}$$

$$\delta V_\pm = (\omega_p/Q_0) D^{-1}(L_1^0 + L_2^0)(L_3^0 + L_4^0) I_\pm , \tag{37b}$$

where

$$\delta v(t) = \mathrm{Re}(\delta V_p e^{j\omega_p t} + \delta V_+ e^{j\omega_+ t} + \delta V_- e^{j\omega_- t}) . \tag{38}$$

Again, the I_0 term in Eq. (37a) drops out upon the balance of inductors. Equation (37b) determines the first-order correction terms to $Z_{\pm 1}$ and $Z_{\pm\pm}$:

$$\delta Z_{\pm 1} = 0 , \tag{39a}$$

$$\delta Z_{\pm\pm} = (\omega_p/Q_0) L_0 \equiv r_0 , \tag{39b}$$

where r_0 is the equivalent resistance in series with the total bridge inductance L_0.

The force equations (16) and (17) remain unchanged upon perturbation. Therefore,

$$\delta F_0 = \delta F_1 = 0 , \tag{40}$$

where

$$\delta f(t) = \mathrm{Re}(\delta F_0 + \delta F_1 e^{j\omega_m t}) . \tag{41}$$

This implies that there is no correction to the reverse transductance:

$$\delta Z_{1\pm} = 0 . \tag{42}$$

One should not conclude from Eq. (40), however, that the input impedance is also unchanged. As we have seen in Sec. III, Z_{11} depends on the output loading condition. The output impedance of the bridge has been modified by Eq. (39b), and we introduce another series resistance r_S to represent the damping in the SQUID input inductance L_S. Combining Eqs. (15b) and (37b), we find

$$V_\pm + \delta V_\pm = \mp(\Lambda I_0 U_1/2)(\omega_\pm/\omega_m) + (j\omega_\pm L_0 + r_0) I_\pm , \tag{43}$$

where the driving voltage is given by the total back emf at the SQUID input:

$$V_\pm + \delta V_\pm = -(j\omega_\pm L_S + r_S) I_\pm . \tag{44}$$

Solving Eq. (43) for $I_\pm$, one finds

$$I_\pm = \pm \frac{1}{j\omega_m (L_0 + L_S)} \left[1 - \frac{r_0 + r_S}{j\omega_\pm (L_0 + L_S)} \right] \frac{\Lambda I_0}{2} U_1 , \tag{45}$$

and, from Eq. (18b),

$$\delta F_1 = \frac{2(r_0 + r_S)}{\omega_p^2 (L_0 + L_S)^2} \left[\frac{\Lambda I_0}{2} \right]^2 U_1 . \tag{46}$$

The ratio $\delta F_1 / U_1$ is the correction to the input impedance

$$\delta Z_{11} = \frac{2}{1+\gamma} \frac{1}{\omega_p L_0 Q_p} \left[\frac{\Lambda I_0}{2} \right]^2 , \tag{47}$$

where

$$Q_p = \omega_p (L_0 + L_S)/(r_0 + r_S) \tag{48}$$

is the electrical Q of the entire circuit, including the SQUID at ω_p.

Notice that δZ_{11} is real and positive, thereby contributing a damping term. Use of Eqs. (32c) and (47) leads to a relationship for the Q's:

$$Q_t^{-1} \equiv [H + \mathrm{Re}(Z_{11})]/M\omega_m = Q_m^{-1} + (\beta_+ + \beta_-) Q_e^{-1} , \tag{49}$$

where H is the mechanical dissipation coefficient, Q_t is the loaded Q of the transducer, and Q_m and Q_e are the mechanical and the electrical quality factors at ω_m, identified as

$$Q_m \equiv M\omega_m / H , \tag{50a}$$

$$Q_e \equiv (\omega_p/\omega_m) Q_p . \tag{50b}$$

The near cancellation of the correction terms in $I_\pm$ is responsible for the reduction of the electrical damping by ω_m/ω_p, the inverse of the parametric gain G_p. This suggests a possibility of virtually eliminating damping at the input signal frequency ω_m.

For the class of dissipation processes which are gov-

erned by the equilibrium thermodynamics, the fluctuations produced by δZ_{11} are taken care of if the perturbed quality factor Q_t, defined above, is used in calculating the Brownian noise of the transducer. Likewise, the additional noise produced by r_0 and r_S at the output of the transducer can be absorbed into the voltage noise of the SQUID by adding their Nyquist noise contribution to S_e in Fig. 1:

$$S_e' = S_e + 4k_B T\omega_p L_0(1+\gamma)Q_p^{-1} . \tag{51}$$

The implication of this additional noise on the gravitational-radiation detector sensitivity is discussed in Sec. V.

V. GRAVITATIONAL-RADIATION DETECTOR SENSITIVITY

The impedance matrix approach to the analysis of the gravitational-radiation detector, advanced by Giffard,[22,23] was originally applied to the case of a noiseless transducer followed by a *voltage* amplifier. This method has been extended by Paik[19,2] to the case in which the transducer is followed by a *current* amplifier. Specifically, noise and optimization of a resonant gravitational-radiation detector employing a resonant passive superconducting transducer followed by a dc SQUID has been analyzed. Here we apply the previous analysis to the detector with an active bridge transducer coupled to a nearly quantum-limited dc SQUID.

In the limit that the transducer noise is unimportant, the "pulse detection noise temperature"[16] of the detector, T_D, can be written in the general form[22,2]

$$T_D = T\frac{\omega_m\tau}{Q_a} + T_N\left[\frac{\alpha_{12}\omega_m\zeta\tau}{2} + \frac{2(\zeta+\zeta^{-1})}{\alpha_{21}\omega_m\tau}\right] , \tag{52}$$

where T and Q_a are the temperature and the quality factor of the antenna; α_{21} and α_{12} are the *forward* and *reverse* signal energy coupling coefficients between the antenna and the amplifier input; T_N and τ are the noise temperature and the integration time of the amplifier. For the case of an *ideal* current amplifier with a zero input impedance, ζ is an impedance matching parameter defined by

$$\zeta \equiv R_{\rm opt}/|Z_{22}| , \tag{53}$$

where $R_{\rm opt}$ and Z_{22} are the optimum source impedance and the output impedance of the transducer, respectively. For a SQUID, the parasitic input impedance $j\omega_{\pm}L_S$ must be added to Z_{22} in Eq. (53). In the case of an active transducer which couples energy through both sideband channels $\omega_{\pm}$, Eq. (52) holds for each sideband. It is convenient, therefore, to interpret the parameters α_{12}, α_{21}, and ζ as the mean values between the two sidebands and describe the combined system with a single expression.

We confine our treatment here to a *resonant* transducer, either in a two-mode[24] or a multimode[25] detector. In such a system, the entire signal energy is transferred to the transducer in half the beat period, $\tau_B/2$. So, if $\tau \gtrsim \tau_B/2$ is chosen, α_{21} and α_{12} reduce to the *mean* transducer energy-coupling coefficients multiplied by a dimensionless factor representing the fraction of the electrical energy coupled to the amplifier input. For our bridge-SQUID system, we have

$$\alpha_{21} = \frac{\gamma}{1+\gamma}\frac{\beta_{+1}+\beta_{-1}}{2} = \frac{\omega_p}{\omega_m}\alpha , \tag{54a}$$

$$\alpha_{12} = \frac{\gamma}{1+\gamma}\frac{\beta_{1+}+\beta_{1-}}{2} = \frac{\omega_m}{\omega_p}\alpha , \tag{54b}$$

$$\alpha \equiv (\alpha_{21}\alpha_{12})^{1/2} = \frac{\gamma}{(1+\gamma)^2}\frac{(\Lambda I_0/2)^2}{M\omega_m^2 L_0} , \tag{54c}$$

where α is the "signal energy-coupling coefficient."

Although transducer noise does not appear explicitly in Eq. (52), one can include the input and output noise contributions from the transducer by redefining Q_a and T_N, as discussed in Sec. IV. In a properly tuned multimode detector, Q_a represents the harmonic mean of the quality factors of all the resonant modes under observation. When electrical coupling is introduced, each of these Q's will be modified according to Eq. (49). The loaded Q of the antenna, Q_a', then must satisfy a similar formula:

$$(Q_a')^{-1} = Q_a^{-1} + 2(1+\gamma)\gamma^{-1}\alpha Q_e^{-1} . \tag{55}$$

In order to account for the output noise of the transducer, we first express T_N and $R_{\rm opt}$ in terms of the equivalent voltage and current noise power spectral densities at the SQUID input, S_e and S_i:

$$T_N = (2k_B)^{-1}(S_e S_i)^{1/2} , \tag{56}$$

$$R_{\rm opt} = (S_e/S_i)^{1/2} , \tag{57}$$

where S_e and S_i are assumed to be uncorrelated. Effective quantities, T_N' $R_{\rm opt}'$, and ζ', can then be defined by substituting S_e' in Eq. (51) for S_e in Eqs. (56), (57), and (53). The transducer noise is properly taken into account if we substitute Q_a', T_N', and ζ' in place of Q_a, T_N, and ζ in Eq. (52).

It has been shown[18,19] for a dc SQUID that

$$R_{\rm opt} = \eta k^2\omega_p L_S , \tag{58}$$

where k^2 is the energy coupling constant of the SQUID input coil L_S and η is a numerical factor of the order of unity, which depends on the operating condition of the SQUID. For a normal operating condition, $\eta \cong 0.4$ has been computed both analytically[19] and numerically.[18] Combining Eq. (58) with Eqs. (56) and (57), one finds

$$S_e = 2k_B T_N \eta k^2\omega_p L_0\gamma , \tag{59a}$$

$$S_i = 2k_B T_N(\eta k^2\omega_p L_0\gamma)^{-1} . \tag{59b}$$

Equation (51) can then be written as

$$S_e' = S_e(1+\xi) , \tag{60}$$

where

$$\xi \equiv \frac{2(1+\gamma)}{\gamma}\frac{1}{\eta k^2 Q_p}\frac{T}{T_N} = \frac{2}{\zeta Q_p}\frac{T}{T_N} , \tag{61}$$

$$\zeta = \gamma(1+\gamma)^{-1}\eta k^2 . \tag{62}$$

It follows from these that

$$T_N' = T_N(1+\xi)^{1/2} , \tag{63}$$

$$\zeta' = \zeta(1+\xi)^{1/2} . \tag{64}$$

We now attempt to minimize T_D. For given antenna and amplifier parameters, the optimum integration time, $\tau_{\rm opt}$, can be shown in a straightforward manner from Eq. (52):

$$\tau_{\rm opt}=\frac{2}{\alpha\omega_m}\left[1+\frac{1}{(\zeta')^2}\right]^{1/2}\left[1+\frac{1}{\alpha Q_a'}\frac{\omega_p}{\omega_m}\frac{2T}{\zeta' T_N'}\right]^{-1/2}, \tag{65}$$

with a corresponding pulse detection noise temperature:

$$T_{D,\rm min}=2T_N'\frac{\omega_m}{\omega_p}[1+(\zeta')^2]^{1/2}\left[1+\frac{1}{\alpha Q_a'}\frac{\omega_p}{\omega_m}\frac{2T}{\zeta' T_N'}\right]^{1/2}. \tag{66}$$

The occurrence of the inverse of the parametric gain, $G_p^{-1}=\omega_m/\omega_p$, in front of T_N' is a manifestation that the active bridge circuit is a *parametric* transducer. In the white-noise range of a SQUID, $T_N\propto\omega_p$ is expected.[18,19] So in the present case, the parametric up conversion is used to move the signal frequency from the $1/f$ noise-dominated region to the white-noise region. For a nearly quantum-limited dc SQUID, this requires $\omega_p/2\pi\gtrsim 100$ kHz. In the limit $T\to 0$, Eq. (66) yields the Giffard limit[22,23] $T_{D,\rm min}=2T_N(\omega_m/\omega_p)$, which becomes $2\hbar\omega_m/k_B$ when T_N is quantum limited. The lowest noise temperature of a dc SQUID has been computed[18,19] to be $T_N\cong 2\hbar\omega_p/k_B$, and such a SQUID has in fact been demonstrated experimentally in the low coupling ($k^2\ll 1$) limit.[14] The best noise temperature of a well-coupled SQUID to date is approximately 60 times worse,[26] judging from its measured flux noise.

With a practical choice $\gamma=1$, which maximizes α, and $k^2\cong 0.5$, ζ is approximately 0.1. In most situations, including the numerical example to be considered in this section, $\xi\lesssim 10$. Therefore, $(\zeta')^2\lesssim 0.1$ from Eq. (64). Equations (65) and (66) can then be simplified, with good approximation, as

$$\tau_{\rm opt}=2(\alpha\omega_m\zeta)^{-1}[A(\alpha,Q_p)]^{-1/2}, \tag{67}$$

$$T_{D,\rm min}=2T_N(\omega_m/\omega_p)[A(\alpha,Q_p)]^{1/2}, \tag{68}$$

where

$$A(\alpha,Q_p)\equiv 1+\frac{2}{\zeta Q_p}\frac{T}{T_N}\left[1+\frac{2(1+\gamma)}{\gamma}+\frac{Q_p}{\alpha Q_a}\frac{\omega_p}{\omega_m}\right]. \tag{69}$$

Since the performance of transducers are the main limitation at present for the sensitivities of the cryogenic gravitational-radiation detectors,[27,9] we compute $\tau_{\rm opt}$ and $T_{D,\rm min}$ as functions of transducer parameters, α and Q_p, given the best antenna and amplifier parameters available today or in the near future.

Figures 4 and 5 show $\tau_{\rm opt}$ and $T_{D,\rm min}$ plotted as functions of α and Q_p. Assumed antenna and amplifier parameters are $T=0.05$ K, $Q_a=10^8$, $\omega_m/2\pi=10^3$ Hz, $\omega_p/2\pi=10^5$ Hz, $\gamma=1$, $\zeta=0.1$, and $T_N=10\hbar\omega_p/k_B=5\times 10^{-5}$ K. For this choice of values, $\xi=2\times 10^4\,Q_p^{-1}$, which satisfies the above condition when $Q_p\gtrsim 2\times 10^3$. In Fig. 4, the limits coming from the beat period in the multimode resonance have been plotted by dashed lines. For an n-mode detector with a mass ratio of μ between the neighboring masses, the beat period can be shown[28] to be

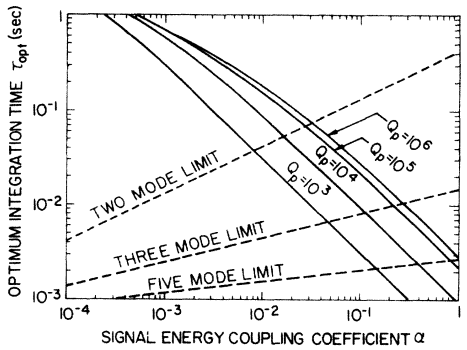

FIG. 4. The optimum integration time $\tau_{\rm opt}$ as a function of transducer parameters α and Q_p.

$$\tau_B=(2\pi/\omega_m)\mu^{1/2}$$
$$=(2\pi/\omega_m)(M_a/M)^{1/[2(n-1)]}, \tag{70}$$

where M_a is the effective mass of the antenna. For the transducer with wire-wound superconducting sensing coils,[5] Λ, I_0, and d_0 (average coil spacing) are practically limited to 1 H m^{-1}, 8 A, and 10^{-4} m, respectively. Equation (54c) then implies an approximate relationship:

$$\alpha\lesssim M_0/M, \tag{71}$$

where $M_0=10^{-3}$ kg. Substituting this into Eq. (70), we obtain the multimode limit:

$$\tau_{\rm min}=\tau_B/2=5\times 10^{-4}\,{\rm sec}(7\times 10^5\alpha)^{1/[2(n-1)]}, \tag{72}$$

where an antenna mass of $2M_a=1.4\times 10^3$ kg is assumed. This limit could be improved by going to thin-film sensing coils. In Fig. 5 the amplifier limit $2T_N(\omega_m/\omega_p)$ and the quantum limit $2\hbar\omega_m$ are indicated by dashed lines.

It appears from these calculations that the transducer parameters required to reach the amplifier limit within a factor of 2 are $Q_p\gtrsim 10^5$ and $\alpha\gtrsim 10^{-2}$. Considering the optimistic assumptions that we have made on the antenna and the amplifier parameters, these transducer parameters appear to be reasonably modest goals. With $\alpha\cong 0.2$ in a three-mode system, one could then have $\tau_{\rm opt}\simeq 10^{-2}$ sec,

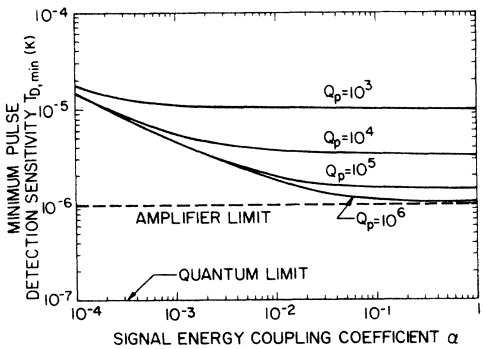

FIG. 5. The minimum pulse detection noise temperature $T_{D,\rm min}$ as a function of transducer parameters α and Q_p.

which corresponds to a detection bandwidth of approximately 50 Hz centered at 1 kHz. The strain sensitivity of this detector is approximately $h_{\min} \cong 4 \times 10^{-20}$, a two-order-of-magnitude improvement over the best sensitivity reported to date.[29]

Throughout this paper, we have assumed that the bridge balance error ϵ_b, defined in Eq. (19), is sufficiently small so that the oscillator noise can be ignored. In practice, ϵ_b is limited by a finite signal-to-noise ratio of the feedback circuit. It is useful, therefore, to derive a condition under which the above sensitivity calculation is valid. If the carrier signal contains sideband components $I_{0,\pm}$, the resulting noise in the output voltage is found from Eq. (15a):

$$\delta V_{p,\pm} \cong \tfrac{1}{4} \epsilon_b j \omega_p L_0 I_{0,\pm} \ . \tag{73}$$

If this quantity is small compared to the signal voltage, the first term in Eq. (15b), the oscillator noise can indeed be ignored. It is straightforward then to obtain the desired condition

$$\epsilon_b (I_{0,\pm}/I_0) < 2x/d_0 \ , \tag{74}$$

where x is the displacement of the transducer proof mass.

With the practical antenna and transducer parameters considered above and with $M_a/M \cong 10^6$, the antenna strain sensitivity $h_{\min} \cong 4 \times 10^{-20}$ with a 50-Hz bandwidth corresponds to the "transducer strain sensitivity" of $x/d_0 \cong 10^{-13}$ Hz$^{-1/2}$. The best available oscillator has an amplitude fluctuation noise of approximately 10^{-8} Hz$^{-1/2}$ at 1 kHz away from a 100-kHz carrier.[30] Substituting these numbers into Eq. (74), we find $\epsilon_b < 10^{-5}$. This in turn requires a signal-to-noise ratio of at least 100 dB in the feedback circuit. These electronic requirements are challenging but appear to be within the state of the art. The balance requirement is relaxed considerably if one used thin-film sensing coils which permit $d_0 \cong 10^{-6}$ m.

VI. CONCLUSIONS

The superconducting inductance-bridge transducer could solve the present difficulties in the passive superconducting transducer. First, a large signal coupling could be obtained in the active device without introducing excessive electrical damping to the mechanical input. Second, the parametric up conversion of the signal frequency will overcome the large $1/f$ noise in nearly quantum-limited dc SQUID's. The relatively poor input coupling constant of the best tunnel-junction dc SQUID's has a modest effect on $T_{D,\min}$ although it has a devastating effect on $\tau_{\rm opt}$ as can be seen from Eqs. (67) and (68). This problem could partially be offset by a large signal coupling constant of the transducer. The poor electrical quality factor of present passive transducers, however, prohibits use of a large transducer coupling. In a parametric transducer with low effective electrical damping, one could utilize α as large as obtainable. A near unity transducer coupling may be realized by going to thin-film coils with a large winding density and a small gap. This new development in the transducer technology, coupled with advances in cooling the antenna to millikelvin temperatures, in wideband detection by means of a multimode detector, and in SQUID technology, may eventually bring us to the standard quantum limit of the resonant-mass gravitational-radiation detector, certainly a desirable milestone before one leaps beyond the quantum limit.[23]

In this paper, we have analyzed a purely inductive bridge. The elimination of capacitance may simplify the bridge balance and minimize the loss in the circuit. Introduction of capacitance would be desirable, however, from the standpoint of high-energy coupling of the transducer. It has been pointed out in Sec. II that a capacitor could be used at the input of the bridge to increase the carrier current without affecting the rest of the circuit. It is also possible to introduce a parallel capacitor at the output of the bridge as a means to increase the output signal coupling to the SQUID, or as a narrow-band filter for one of the sidebands in case a nonsymmetric detection of the sidebands is desirable. Application of the back-action evasion method,[31,32] for example, may require introduction of additional capacitances into the system, as in the scheme of Bocko and Johnson.[33] The basic scheme analyzed in this paper, however, has the merit of simplicity and is worth experimental investigation.

ACKNOWLEDGMENTS

I wish to acknowledge useful discussions with J. W. Parke, H. A. Chan, M. V. Moody, W. M. Fairbank, P. F. Michelson, and T. R. Stevenson. This work was supported in part by National Science Foundation Grant No. PHY82-15218.

*Permanent address: Department of Physics and Astronomy, University of Maryland, College Park, MD 20742.

[1]J. Weber, Phys. Rev. **117**, 306 (1960).

[2]For classification and general analytical treatment of transducers used for gravitational-radiation detectors, see H. J. Paik, in *Proceedings of the Second Marcel Grossmann Meeting on General Relativity,* edited by R. Ruffini (North-Holland, Amsterdam, 1982), p. 1193.

[3]J.-P. Richard, Rev. Sci. Instrum. **47**, 423 (1976).

[4]K. Narihara and H. Hirakawa, Jpn. J. Appl. Phys. **15**, 833 (1976).

[5]H. J. Paik, J. Appl. Phys. **47**, 1168 (1976).

[6]V. B. Braginsky, in *Experimental Gravitation,* edited by B. Bertotti (Academic, New York, 1974), p. 235.

[7]D. G. Blair, Rev. Sci. Instrum. **50**, 286 (1979).

[8]W. C. Oelfke and W. O. Hamilton, Acta Astronaut. **5**, 87 (1978).

[9]D. G. Blair, in *Gravitational Radiation, Collapsed Objects and Exact Solutions,* edited by C. Edwards (Springer, Berlin, 1980), p. 314.

[10]V. B. Braginsky, in *Proceedings of the International Symposium on Experimental Gravitation* (Academia Nazionale dei Lincei, Rome, 1977), p. 219.

[11]H. Hirakawa, *Proceedings of the International Symposium on Experimental Gravitation* (Ref. 10) p. 227.

[12]H. J. Paik, Ph.D. thesis, Stanford University, Stanford, Cali-

fornia, 1974 (unpublished).
[13]W. W. Johnson and M. Bocko, Phys. Rev. Lett. **47**, 1184 (1981).
[14]D. J. Van Harlingen, R. H. Koch, and J. Clarke, Appl. Phys. Lett. **41**, 197 (1981).
[15]R. P. Giffard and H. J. Paik, Stanford University report, 1977 (unpublished). This paper has been reproduced with slight modification in Ref. 9.
[16]P. F. Michelson and R. C. Taber, Phys. Rev. D **29**, 2149 (1984).
[17]J. N. Hollenhorst, Ph.D. thesis, Stanford University, Stanford, California, 1979 (unpublished).
[18]J. Clarke, C. D. Tesche, and R. P. Giffard, J. Low Temp. Phys. **37**, 405 (1979).
[19]H. J. Paik, Nuovo Cimento **55B**, 15 (1980).
[20]Y. B. Kim and M. J. Stephen, in *Superconductivity,* edited by R. D. Parks (Marcel Dekker, New York, 1969), p. 1107.
[21]B. W. Ricketts, J. Phys. E **9**, 179 (1976).
[22]R. P. Giffard, Stanford University report, 1975 (unpublished). This paper has been reproduced in its original form by Blair, in *Gravitational Radiation, Collapsed Objects and Exact Solutions* (Ref. 9), p. 299.
[23]R. P. Giffard, Phys. Rev. D **14**, 2478 (1976).
[24]H. J. Paik, in *Experimental Gravitation* (Ref. 6), p. 515.
[25]J.-P. Richard, in *Gravitational Radiation, Collapsed Objects and Exact Solutions* (Ref. 9), p. 370.
[26]M. B. Ketchen and J. M. Jaycox, Appl. Phys. Lett. **40**, 736 (1982).
[27]P. F. Michelson and R. C. Taber, J. Appl. Phys. **52**, 165 (1981).
[28]J.-P. Richard, Phys. Rev. Lett. **52**, 165 (1984).
[29]S. P. Boughn, W. M. Fairbank, R. P. Giffard, J. N. Hollenhorst, E. R. Mapoles, M. S. McAshan, P. F. Michelson, H. J. Paik, and R. C. Taber, Astrophys. J. **261**, L19 (1982).
[30]*Crystal Oscillators,* catalog from Vectron Laboratories, Inc., Norwalk, Connecticut (1985).
[31]V. B. Braginsky and A. B. Manukin, in *Measurement of Weak Forces in Physics Experiments,* edited by D. H. Douglass (University of Chicago Press, Chicago, 1977).
[32]C. M. Caves, K. S. Thorne, R. W. P. Drever, M. Zimmerman, and V. D. Sandberg, Phys. Rev. Lett. **40**, 667 (1978).
[33]M. Bocko and W. W. Johnson, Phys. Rev. Lett. **48**, 1371 (1982).